BIODIVERSITAS
Volume 25, Number 7, July 2024
Pages: 3179-3192

ISSN: 1412-033X
E-ISSN: 2085-4722
DOI: 10.13057/biodiv/d250739

Phytochemical, antioxidant, and in-silico studies of *Erigeron sumatrensis* from Gayo Highlands, Indonesia as a potential inhibitor of Type-2 diabetes mellitus

VIVERA RUSELLI PUSPA[1,2], ZUMAIDAR[3,♥], NURDIN[4], FITMAWATI[5]

[1]Department of Biology Education, Faculty of Teacher Training and Education, Universitas Syiah Kuala. Jl. Tgk Hasan Krueng Kalee, Banda Aceh 23111, Aceh, Indonesia
[2]Graduate School of Mathematics and Applied Sciences, Universitas Syiah Kuala. Jl. Tgk Chik Pante Kulu No. 5, Banda Aceh 23111, Aceh, Indonesia
[3]Department of Biology, Faculty of Mathematics and Natural Sciences, Universitas Syiah Kuala. Jl. Syech Abdurrauf No. 3, Banda Aceh 23111, Aceh, Indonesia. Tel.: +62-651-7410248, Fax.: +62-651-755138, ♥email: zumaidar@usk.ac.id
[4]Department of Chemistry, Faculty of Mathematics and Natural Sciences, Universitas Syiah Kuala. Jl. Syech Abdurrauf No. 3, Banda Aceh 23111, Aceh, Indonesia
[5]Department of Biology, Faculty of Mathematics and Natural Sciences, Universitas Riau. Jl. H.R Soebrantas Km. 12,5, Kampus Bina Widya Simpang Baru, Pekanbaru 28293, Riau, Indonesia

Manuscript received: 19 March 2024. Revision accepted: 19 July 2024.

Abstract. *Puspa VR, Zumaidar, Nurdin, Fitmawati. 2024. Phytochemical, antioxidant, and in-silico studies of* Erigeron sumatrensis *from Gayo Highlands, Indonesia as a potential inhibitor of type-2 diabetes mellitus. Biodiversitas 25: 3179-3192. Erigeron sumatrensis* Retz., a wild medicinal herb, was determined qualitatively and quantitatively for its leaf extract's phytochemical constituents and antioxidant capacity and to conduct computational studies. Secondary metabolites identified included flavonoids, phenolics, terpenoids, steroids, and alkaloids. The methanol fraction exhibited the greatest TPC (5945.45 mg GAE/g). Antioxidant activity, as determined by the ABTS assay, indicated a significant radical scavenging activity in the methanol fraction of *E. sumatrensis* leaves, with an IC_{50} value of 57.67 µg/mL. In silico molecular docking revealed that cucurbitacin b, 25-desacetoxy-β-sitosterol, and α-amyrin exhibited potential as α-glucosidase inhibitors (PDB ID: 2QMJ). The same compounds demonstrated inhibitory properties against α-amylase (PDB ID: 2QV4), with acarbose as a positive control with a binding energy of -7.8 kcal/mol. The ADMET profiles indicated compliance with Lipinski's rule of five for all compounds, suggesting their suitability as an orally administered drug. Based on these findings, *E. sumatrensis* has excellent potential as a source of raw materials for antidiabetic drug formulation, so it needs to be further investigated for pharmaceutical applications.

Keywords: Antioxidant**,** *Erigeron sumatrensis,* Gayo highlands, molecular docking, phytochemical

Abbreviation: T2DM: Type-II Diabetes Mellitus; TPC: Total Phenolic Content; TFC: Total Flavonoid Content; TTC: Total Tannin Content; GC-MS: Gas Chromatography-Mass Spectrometry; DPPH: 1,1 diphenyl-2-picrylhydrazyl; ADMET: Absorption, Distribution, Metabolism, Excretion, and Toxicity; PDB ID: Protein Data Bank Identification; IC_{50}: The half-maximal inhibitory concentration; RCSB: Research Collaboratory for Structural Bioinformatics; GI: Gastrointestinal; LOAEL: Lowest Observed Adverse Effect Level; BBB: Blood-Brain Barrier; P-gp: P-glycoprotein; LD_{50}: Lethal Dose 50; VDss: The Volume of Distribution at Steady State

INTRODUCTION

Diabetes Mellitus (DM) represents a pervasive chronic condition with an increasing global incidence rate. The disease manifests through sustained hyperglycemia, so the body cannot metabolize to energy production, coupled with perturbations in the metabolic regulation of proteins, lipids, and carbohydrates. Beyond elevated blood glucose levels, diabetes mellitus may predispose individuals to various complications, encompassing microvascular and macrovascular damage, neuropathic disorders, and heightened mortality risks. DM can be categorized into Type 1 (T1DM) and Type-2 (T2DM), accounting for 90-95% of cases. The prevalence of T2DM is experiencing a substantial annual increase, as confirmed in the research conducted by Chipiti et al. (2017).

The Gayo Highlands is a region that has significant potential for the Asteraceae. It can be seen in the biodiversity present along most provincial highways and residential areas. The flourishing of Asteraceae floral species within these highland areas can be attributed to environmental conditions that support their growth (Nikolić and Stevović 2015; Asif et al. 2020; Zhao et al. 2020). Although wild Asteraceae are frequently classified as weeds due to their spontaneous emergence, they possess substantial traditional medicinal potential. Locally, these plants are utilized as herbal medicine and biological agents, so they have high economic value (Bartolome et al. 2013; Abu-Izneid et al. 2020). The community engages in the therapeutic application of these plants as alternative medicine, often unaware of the specific phytochemical compounds they contain (Rolnik and Olas 2021). The ethnopharmacological aspects of Asteraceae have garnered research attention, as evidenced by studies from Fu et al. (2021) and Rustaiyan and Faridchehr (2021), studied the ethnopharmacological aspects of the Asteraceae revealed that several species of the

Asteraceae serve as valuable raw materials in various applications (Ascari et al. 2019; González-Zamora et al. 2020; Al-Momani et al. 2023; Jhariya and Pawar 2024).

Phytochemical screening and bioassay are preliminary evaluations to determine the plant's therapeutic effects. The phytochemical examination aims to identify plant-secondary metabolites that may harbor pharmaceutical potential (Soković et al. 2019; Ernilasari et al. 2021). Concurrently, bioassay screening functions as a foundational assessment to predict the bioactivity of plant species. Exploring novel therapeutics derived from natural products remains a critical priority in contemporary research.

Recent technological advances have increased the use of computational methods for drug discovery, as they significantly reduce costs and time requirements (Al-Qahtani et al. 2023; Erukainure et al. 2023). The in-silico approach is a powerful computational instrument, facilitating the prediction and formulation of hypotheses, potentially leading to novel findings or advancements in the medical and healthcare fields. Furthermore, in-silico methods support decision-making by enabling the virtual simulation of almost every aspect of drug discovery and development (Lopes et al. 2013; Ahmed et al. 2022). Applying in-silico techniques allows the screening of therapeutic properties in a virtual environment, thereby reducing the necessity for animal testing in pharmacology and subsequent ethical concerns. Additionally, these computational predictions generate candidate compounds that can provide a basis for extensive in vivo and in vitro research.

Erigeron sumatrensis, syn. *Conyza sumatrensis*, regionally known as Jelantir, is commonly found in the Gayo Highlands. Related species, such as *Conyza bonariensis*, had a 94.57% inhibition rate at a concentration of 0.05 mg/mL and an IC_{50} value of 4.93±0.15 µg/mL, indicating a more potent antioxidant capacity than the ascorbic acid control (IC_{50} 5.21±0.05 µg/mL) (Thabit et al. 2015). Due to its close taxonomic relationship with *C. bonariensis*, *E. sumatrensis* is hypothesized to possess antioxidant potential. The comprehensive phytochemical potential of *E. sumatrensis* remains underexplored. The phytochemical compositions of several Asteraceae species have been previously characterized (Bakar et al. 2015; Ali et al. 2017; Ascari et al. 2019; Soleimani et al. 2019; González-Zamora et al. 2020; Javeed et al. 2022; Ruiz-Reyes et al. 2022; Timalsina and Devkota 2022). Phytochemical screening of *E. sumatrensis* from the Gayo Highlands has yet to be conducted. An in-silico examination of leaf extracts of *E. sumatrensis* could provide valuable insights into its phytochemical composition, antioxidant capabilities, and antidiabetic properties.

MATERIALS AND METHODS

Collection and extraction of *Erigeron sumatrensis* leaves

Leaves of *E. sumatrensis* were collected during the period of 09:00 to 13:00 in July 2023 within Suka Makmur Village boundaries, located in the Wih Pesam Sub-district of the Bener Meriah District, Aceh Province, Indonesia (Figure 1). Taxonomic verification and species confirmation were carried out at the Biology Education Laboratory of the Universitas Syiah Kuala under the auspices of the Faculty of Teacher Training and Education. A total of 8 kilograms of freshly harvested leaves were cleaned with water, followed by a careful crushing process. Then, the plant material was air-dried for seven days and underwent a sequential maceration procedure. Subsequently, 2 kg of simplicia powder was macerated in various solvents, i.e., 70% *n*-hexane, 70% ethyl acetate, and 96% methanol. The filtrates were then concentrated under reduced pressure utilizing a vacuum rotary evaporator at 40°C to 50°C (Truong et al. 2019; Suoth et al. 2022).

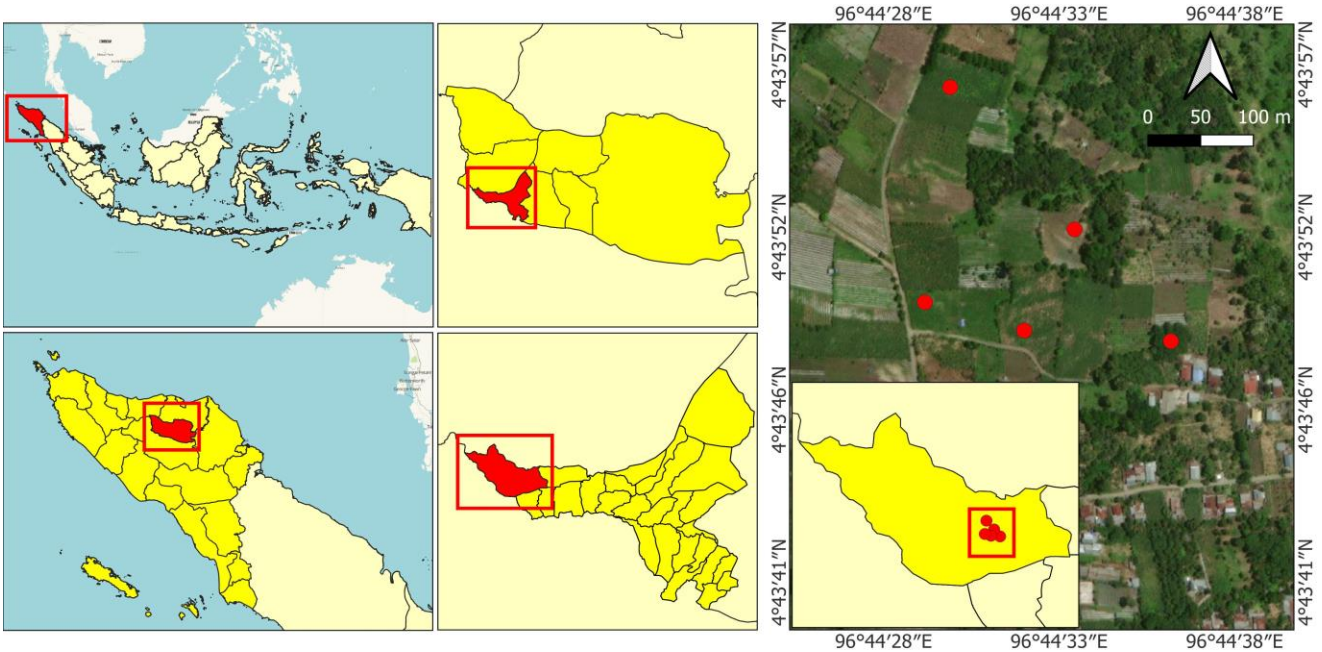

Figure 1. Five sampling sites of *Erigeron sumatrensis* in Suka Makmur Village, Wih Pesam Sub-district, Bener Meriah District, Aceh, Indonesia

Procedure

Phytochemical test

A qualitative phytochemical assessment was conducted on the hexane, ethyl acetate, and methanol extract of *E. sumatrensis* leaves. This analysis includes flavonoids, phenolics, terpenoids, steroids, tannins, saponins, and alkaloids. The procedures followed the method by Nuraskin et al. (2020).

Total Flavonoid Content (TFC)

Total flavonoid content (TFC) was analyzed using a colorimetric method by Phuyal et al. (2020), with quercetin as the reference compound. 5 mg of the extract was dissolved in 5 mL of methanol p.a. Subsequently, 1 mL of this solution was mixed with 3 mL of methanol, 0.2 mL of $AlCl_3$, 0.2 mL of potassium acetate, and 5.6 mL of deionized water. The same procedure was applied to quercetin. Dilution was carried out to generate a concentration series of 100, 125, 150, 175, and 200 ppm. After that, 1 mL of each concentration from the series was mixed with 3 mL of methanol p.a, 0.2 mL of $AlCl_3$, 0.2 mL of potassium acetate, and 5.6 mL of distilled water. Post-incubation for 30 minutes at ambient temperature (25°C), the absorbance of each solution was measured utilizing a UV-Vis spectrophotometer (Shimadzu 206-24000-92 Uvmini-1240, Kyoto, Japan) at a wavelength of 510 nm (Farahmandfar and Ramezanizadeh 2018). The total flavonoid content was expressed as mg quercetin equivalent per gram of extract (mg QE/g extract). This assay was performed in triplicate for all samples.

Total Phenolic Content (TPC)

The total phenolic content in the extracts was determined by the Folin-Ciocalteu reagent method. Initially, 5 mg of the extract was dissolved in 0.5 mL methanol p.a and diluted with deionized water to a final volume of 5 mL. To 0.2 mL of this dilution, 15.8 mL deionized water and 1 mL Folin-Ciocalteu reagent were added. The reaction was continued by adding 3 mL of a 10% (w/v) Na_2CO_3 solution after 5 minutes of incubation, followed by incubation for 120 minutes at room temperature. Concurrently, a calibration curve was established using 5 mg of gallic acid dissolved in 1 mL methanol p.a. and then added with deionized water to 10 mL. A series of dilutions were prepared to create standard concentrations of gallic acid (100 µg/mL, 125 µg/mL, 150 µg/mL, 175 µg/mL, and 200 µg/mL). 0.2 mL from each concentration was mixed with 15.8 mL of deionized water and 1 mL of the Folin-Ciocalteu reagent. After incubating for 5 minutes, 3 mL of 10% (w/v) Na2CO3 was added to this mixture and incubated again for 120 minutes at ambient temperature. The absorbance was then measured using a UV-Vis spectrophotometer at a wavelength of 765 nm, as cited by Indriaty et al. (2023). The total phenolic content was quantified as mg gallic acid equivalent per gram of extract (mg GAE/g extract). The analysis was carried out in triplicate.

Total Tannin Content (TTC)

The total tannin content was performed using an established standard method by Sadeer et al. (2019). Aliquots consisting of 1 mL of sample solutions at a concentration of 1000 ppm were added with 0.5 mL of Folin-Ciocalteu reagent. Subsequently, the samples were saturated with a 35% sodium carbonate solution and added with 8 mL of distilled water. The mixtures were then allowed to equilibrate at room temperature for 30 minutes. Post incubation, the optical density of the supernatant was measured at a wavelength of 725 nm through a UV-visible spectrophotometer. Tannic acid was used as the calibration standard. The content of tannins was expressed as mg tannic acid equivalent per 10 mg of sample (mg TAE/g extract), as detailed by Frederick and Mani (2016). The analysis was conducted in triplicate.

Gas Chromatography-Mass Spectrometry (GC-MS) analysis

The methanolic extract of *E. sumatrensis* leaves had the most significant antioxidant activity. Therefore. It was selected for subsequent GC-MS analysis following the method reported by Masyudi et al. (2022). The GC-MS investigations were performed using an Agilent Technologies 7890A GC system equipped with a 5975A MSD and an Auto Sampler alongside a Chemstation data system for chromatographic analysis. 5 µL of sample in methanol was injected into the GC-MS. Helium was the carrier gas with a 1.2 mL/min flow rate and a split ratio of 8:1 psi. The injector and detector temperatures were set at 250°C and 230°C, respectively, with the column oven temperatures programmed to 280°C and 140°C. The reference data provided by The National Institute of Standards and Mass Spectral Technology (NIST-MS) database facilitated the interpretation of the mass spectral fragmentation patterns.

Antioxidant DPPH (1,1 diphenyl-2-picrylhydrazyl

Antioxidant activity was evaluated using the 2.2-diphenyl-1-picrylhydrazyl free radical scavenging assay by Yahya et al. (2021). 2.5 mg of the extract was mixed with two drops of 2% dimethyl sulfoxide to increase solubility, and the extract was allowed to rest for 24 hours. After that, the extracts were diluted at concentrations ranging from 1.56, 3.125, 6.25, 12.5, 25, 50, and 100 mg/mL in methanol p.a and homogenized using a sonicator, following the protocols described by Furi et al. (2020). A volume of 4 mL of the solution was combined with 1 mL of a freshly prepared DPPH solution derived from dissolving 7.9 mg of DPPH powder in 5 mL of methanol p.a. This mixture was homogenized and incubated in the dark at 37°C for 30 minutes. Spectrophotometric absorbance readings were taken at 517 nm, with methanol p.a. as the blank reference. Ascorbic acid was used as a positive control, replicated with 1 to 15 g/mL concentrations. Furthermore, the inhibition percentage of DPPH radicals was calculated to determine the IC_{50} value, namely the extract concentration needed to scavenge half of the DPPH radical. Those extract samples demonstrating superior antioxidant properties were then subjected to Gas Chromatography-Mass Spectrometry analysis (Shimadzu QP2000A, Kyoto, Japan) for the determination of their phytoconstituents (Nurmilasari et al. 2017; Indriaty et al. 2023).

Increasing DPPH free radical scavenging activity is inversely correlated with decreasing DPPH solution's

absorbance. The quantification of free radical scavenging activity, expressed as the percentage of inhibition, is determined using the following formula (Boucheffa et al. 2022).

$$\text{Inhibition (\%)} = \frac{(\Delta A_{\text{Control}} - \Delta A_{\text{Sample}})}{\Delta A_{\text{Control}}} \times 100$$

The antioxidant activity data were processed and analyzed utilizing Microsoft Excel 2010. The half-maximal inhibitory concentration for the antioxidant assay was deduced by conducting a linear regression analysis, which related the sample concentration (expressed in µg/mL) to the percentage of radical inhibition

Antioxidant activity based on FRAP (Ferric Reducing Antioxidant Power) assay

The Ferric-Reducing Antioxidant Power (FRAP) assay was conducted using the analytical methodology outlined by Raharjo et al. (2023). An aliquot of 1 mL of each of methanol, ethyl acetate, and *n*-hexane extracts of *E. sumatrensis* leaves at 5, 10, 25, 50, and 100 ppm was combined with 1 mL of phosphate-buffered saline at pH 6.6, and 1 mL of potassium ferricyanide [K_3Fe_6]. The mixtures were then incubated at 50°C for 20 minutes. Following incubation, 1 mL of trichloroacetic acid was added. The reaction mixture was then centrifugated at 3000 rpm for a 10-minute. Subsequently, 1 mL of supernatant was added with 1 mL of distilled water and 0.5 mL of 0.1% FeCl3 solution. The resulting solution was incubated for a specific time, after which the absorbance was measured at the maximum wavelength.

Antioxidant activity based on ABTS (2,20-azino-bis(3-ethylbenzothiazoline-6-sulfonic acid) assay

The ABTS analysis was carried out strictly according to the method by Tangkau et al. (2023). The ABTS assay consisted of several steps as follows:

Stock solution of *E. sumatrensis* extract. A stock solution of 1000 ppm was prepared using the following procedure: 50 mg of *E. sumatrensis* leaf extract was accurately weighed and dissolved in methanol. This solution was homogenized, and methanol was added to reach the final volume of 50 mL within a volumetric flask.

Preparing a concentrated solution of vitamin C. A solution of vitamin C at a concentration of 1000 ppm was performed by precision weighing 10 mg of pure vitamin C p.a., which was then dissolved in methanol to the mark of 10 mL in the volumetric flask.

Preparing a 7 mM stock solution of ABTS. Solution A was prepared by precisely weighing 0.385 g of 2,2'-azino-bis(3-ethylbenzothiazoline-6-sulfonic acid) and dissolving it in 100 mL of distilled water. At the same time, solution B was created by accurately weighing 0.066 g of potassium persulfate ($K_2S_2O_8$) and dissolving it in 100 mL of distilled water. The two solutions were combined under reduced light conditions and were added with analytical-grade methanol to the desired volume. The resultant mixture was subsequently incubated at room temperature (25°C) for a period ranging from 12 to 16 hours.

Determination of Operating Time (OT). 0.1 mL of ABTS solution was placed into a 5.0 mL volumetric flask. Subsequently, 1 mL of a 4 ppm vitamin C solution was added to the flask. The absorbance of the mixture was measured at 750 nm wavelength, with readings taken at one-minute intervals until a stable absorbance was reached.

Determination of the wavelength of peak absorption. A 0.1 mL aliquot of the ABTS solution was dispensed into a 5.0 mL volumetric flask containing 4 ppm of vitamin C. The absorbance of this mixture was measured using a UV-visible spectrophotometer calibrated to a wavelength range of 700-750 nm, intended to identify the wavelength of peak absorption.

Measurement of ABTS free radical binding activity using pure C. 10 mg of analytical-grade vitamin C was solubilized in 10 mL of methanol to yield a stock solution of 1000 ppm. Aliquots of 1.6 mL, 2 mL, 2.4 mL, 2.8 mL, and 3.2 mL of the stock solution were carefully drawn. These aliquots were then diluted with methanol to a total volume of 10 mL, resulting in final concentrations of 8 ppm, 10 ppm, 12 ppm, 14 ppm, and 16 ppm, respectively. For analytical purposes, 0.1 mL from each concentration was transferred into a test tube, to which 2 mL of the ABTS reagent and 4 mL of methanol were subsequently added. The solutions were left to incubate at ambient temperature for 30 minutes. Post-incubation, the absorbance of each solution at 750 nm was recorded. This measurement procedure was replicated thrice to ensure the reliability of the results.

Measurement of ABTS free radical scavenging activity of extract. A precisely measured 10 mg of *E. sumatrensis* leaf extract was dissolved in 10 ml methanol in a 10 mL volumetric flask, resulting in a stock solution of 1000 ppm concentration. Subsequently, solutions with concentrations of 8 ppm, 10 ppm, 12 ppm, 14 ppm, and 16 ppm were prepared based on the standard dilution formula.

$$M_1 . V_1 = M_2 . V_2$$

For each specified concentration, a 0.1 mL aliquot was dispensed using a pipette into a test tube, to which 2 mL of ABTS reagent and 4 mL of methanol were added, bringing the total volume of the solution to 6.1 mL. This solution was then allowed to equilibrate at room temperature for 30 minutes. The absorbance for each sample was determined at a wavelength of 750 nm. This measurement was conducted in triplicate to ensure experimental precision.

In-silico study (molecular docking)

The elucidated crystal structures of the α-glucosidase (Protein Data Bank [PDB] ID: 2QMJ) and α-amylase (PDB ID: 2QVA) proteins were acquired from the Research Collaboratory for Structural Bioinformatics Protein Data Bank (RCSB PDB) (https://www.rcsb.org/) to conduct molecular docking studies. Concurrently, ligands identified from Gas Chromatography-Mass Spectrometry analyses were retrieved from the PubChem database. Prior to docking, ligand candidates were evaluated for their drug-like properties following Lipinski's Rule of Five, utilizing the Swiss ADME online tool (http://www.swissadme.ch/). Subsequently, the PyMol 2.5.5 software was used to excise water molecules and superfluous atoms from the crystallographic

data, thus producing files in the (.pdb) format. These files, representing both ligands and receptors, underwent preparation via Autodock Tools 1.5.6 for the consolidation of non-polar hydrogens, the addition of polar hydrogens, and the conversion to the docking-compatible file format (.pdbqt) (Valdés-Tresanco et al. 2020).

Molecular screening was conducted using the PyRx 0.8 software, which utilizes the Autodock Vina engine for molecular docking simulations. During these simulations, ligand molecules were treated as flexible, while the protein targets were kept rigid, and all entities were in the (.pdbqt) file format. Grid parameters for the docking process were generated through the PyRx Auto Grid feature, which creates specific configuration files. Additionally, PyRx 0.8 facilitated the identification of amino acid residues within the protein's active site that interact with the ligand molecules. Compounds exhibiting the most negative binding affinity values, indicative of the highest binding energy, were deemed optimal candidate compounds (Chandel et al. 2022). After docking, the PyMol 2.5.5 software was utilized to visualize the receptor-ligand complexes, saving the outputs in the (.pdb) file format. For a comprehensive analysis of these interactions, both in two and three dimensions, the BIOVIA Discovery Studio 2021 software read the receptor-ligand interaction files (.pdb), facilitating the examination of the binding phenomena.

In-silico study (ADMET)

Optimal compounds identified through docking were subjected to an absorption, distribution, metabolism, excretion, and toxicity profile assessment utilizing the Swiss ADME online resource. This evaluation was conducted to ascertain the compounds' pharmacokinetic properties and potential bioavailability (Majid et al. 2022). Furthermore, the compounds demonstrating favorable docking outcomes were evaluated for toxicity employing the pkCSM online tool (https://biosig.lab.uq.edu.au/pkcsm/prediction), thereby providing insights into their overall suitability and safety for further development (Gholam and Artika 2023).

RESULTS AND DISCUSSION

Phytochemical profiling of extract

Phytochemical analyses conducted on *n*-hexane, ethyl acetate, and methanol extracts derived from the leaves of *E. sumatrensis* revealed the presence of several bioactive constituents, including flavonoids, phenolics, terpenoids, steroids, and alkaloids (Table 1).

Total bioactive contents

The total flavonoids, phenolics, and tannins content of the *E sumatrensis* extract are presented in Table 2.

Determination of phytochemicals by GC-MS

Analysis of antioxidant activity revealed that the methanol fraction exhibited the highest potency. Consequently, this fraction was selected for further analysis via gas chromatography-mass spectrometry to elucidate its chemical composition. GC-MS analysis was conducted to elucidate major and minor phytochemical constituents present in the methanol fraction extract of *E. sumatrensis* leaves. This analysis used a silica capillary column to separate individual components and identified. Twenty-eight compounds were tentatively characterized and identified based primarily on the relative peak areas depicted in the chromatogram. Predominant phytoconstituents such as phytol (19.32%), lupeol (17.68%), β-sitosterol (10.58%), methyl 8,11,14-heptadecatrienoate (4.52%), farnesyl bromide (4.41%), 2-methoxy-4-vinylphenol (3.63%), α-amyrin (3.45%), and caryophyllene oxide (3.11%) were identified, along with various other minor compounds. These compounds encompassed several classes, including triterpenoids, sesquiterpenoids, phenols, sterols, esters, and alcohols, as presented in Table 3. It is important to note that triterpenoids have significant therapeutic potential (Sohag et al. 2022).

Antioxidant activities

Table 4 presents the antioxidant capacities of the *n*-hexane, ethyl acetate, and methanol extracts from *E. sumatrensis.*

Table 1. Phytochemical analysis of the extract of *Erigeron sumatrensis* leaves in various solvents

Secondary metabolites	*n*-hexane	Ethyl acetate	Methanol
Flavonoids	-	+	+
Phenolic	-	+	+
Terpenoids	+	+	+
Steroids	+	+	+
Tannin	-	-	-
Saponin	-	-	-
Alkaloids			
Dragendorff	-	+	+
Mayer	-	+	+
Wagner	-	+	+

Note: (+): present; (-): absent

Table 2. Total flavonoid, total phenolic, and tannin content of *Erigeron sumatrensis* leaves

Fractions	Total bioactive content		
	TFC (mg QE/g)	TPC (mg GAE/g)	TTC (mg TAE/g)
n-hexane	86.92	1581.82	6.36
Ethyl acetate	631.15	5763.64	92.72
Methanol	1017.69	5945.45	274.54

Note: TFC: Total Flavonoid Content; TPC: Total Phenolic Content; TTC: Total Tannin Content

Table 3. Identified metabolites of leaves methanol extract of *Erigeron sumatrensis* by GC-MS

Peak number	Retention time (minutes)	SI	Peak areas (%)	Phytochemical identified compounds	Molecular formula	Class
1.	18.94	699	3.63	2-Methoxy-4-vinylphenol	$C_9H_{10}O_2$	Phenol
2.	20.06	644	1.88	Phenol, 2-methoxy-5-(1-propenyl)-, (E)-	$C_{10}H_{12}O_2$	Phenol
3.	22.49	740	1.48	cis-ß-Farnesene	$C_{15}H_{24}$	Sesquiterpenoids
4.	25.55	861	2.72	1H-Cycloprop[e]azulen-7-ol, decahydro- 1,1,7-trimethyl-4-methylene-, [1ar- (1aa,4aa,7ß,7aß,7ba)]-	$C_{15}H_{24}O$	Sesquiterpenoids
5.	25.7	816	3.11	Caryophyllene oxide	$C_{15}H_{24}O$	Sesquiterpenoid oxide
6.	27.36	691	1.58	2,3-Dehydro-4-oxo-ß-ionol	$C_{13}H_{18}O$	Ketones
7.	27.64	753	0.69	trans-Za-Bisabolene epoxide	$C_{15}H_{24}O$	Sesquiterpenoids
8.	27.79	704	1.97	Z-3-Hexadecen-7-yne	$C_{16}H_{28}$	Alkynes
9.	30.99	785	1.96	E-2-Tetradecen-1-ol	$C_{14}H_{28}O$	Alcohol
10.	31.13	710	0.81	Pterin-6-carboxylic acid	$C_7H_5N_5O_3$	Pterin
11.	32.72	749	2.93	Hexadecanoic acid, methyl ester	$C_{17}H_{34}O_2$	Ester
12.	34.74	669	2.84	Taylorione	$C_{15}H_{22}O$	Sesquiterpenoids
13.	35.29	643	2.90	1,4-Cyclohexanediol, (Z)-, TMS derivative	$C_6H_{12}O_6$	Hexahidrokuinon
14.	35.91	773	1.14	Methyl 9-cis,11-trans-octadecadienoate	$C_{19}H_{34}O_2$	Ester
15.	36.03	825	4.52	Methyl 8,11,14-heptadecatrienoate	$C_{18}H_{30}O_2$	Ester
16.	36.24	900	19.32	Phytol	$C_{20}H_{40}O$	Diterpenoids
17.	38.09	745	1.93	E-2-Tetradecen-1-ol	$C_{14}H_{28}O$	Alcohol
18.	49.99	688	4.41	Farnesyl bromide	$C_{15}H_{25}Br$	Haloalkanes
19.	50.86	658	1.36	Cucurbitacin b, 25-desacetoxy-	$C_{30}H_{44}O_6$	Cucurbitan
20.	51.12	660	1.10	9,10-Secocholesta-5,7,10(19)-triene-3,24,25- triol, (3ß,5Z,7E)-	$C_{27}H_{44}O_3$	Sterols
21.	51.51	644	0.92	9,10-Secocholesta-5,7,10(19)-triene-3,24,25- triol, (3ß,5Z,7E)-	$C_{27}H_{44}O_3$	Sterols
22.	51.64	646	0.77	9,10-Secocholesta-5,7,10(19)-triene-3,24,25- triol, (3ß,5Z,7E)-	$C_{27}H_{44}O_3$	Sterols
23.	54.06	735	10.58	ß-Sitosterol	$C_{29}H_{50}O$	Triterpenoids
24.	54.39	724	17.68	Lupeol	$C_{30}H_{50}O$	Triterpenoids
25.	54.66	728	3.45	a-Amyrin	$C_{30}H_{48}O_2$	Triterpenoids
26.	54.83	672	0.87	Lupeol	$C_{30}H_{50}O$	Triterpenoids
27.	55.40	699	2.86	a-Amyrin	$C_{30}H_{48}O_2$	Triterpenoids
28.	58.66	618	0.58	W-18	$C_{19}H_{20}ClN_3O_4S$	Analgesic

Note: SI: Similarity Index

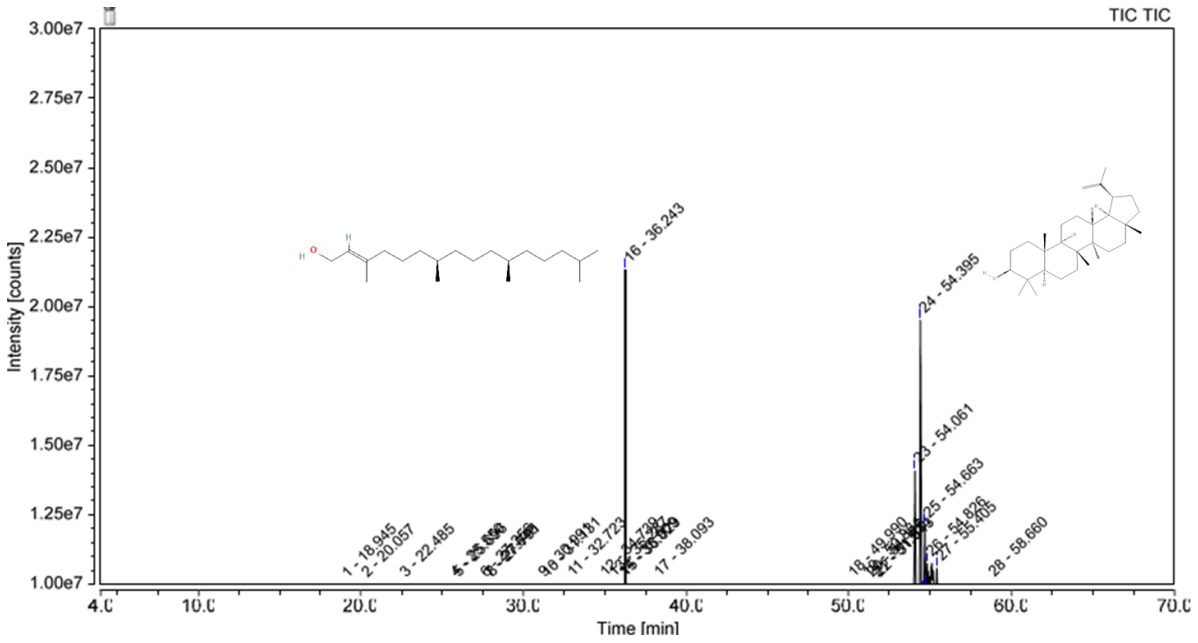

Figure 2. GC-MS chromatogram of methanol fractions extract of *Erigeron sumatrensis* leaves

In-silico study

Molecular docking

Molecular docking studies were conducted to ascertain the nature and bonding interactions between the targeted enzymes (α-glucosidase and α-amylase) and ligands, as identified through GC-MS analysis (referenced in Table 3). The computed binding affinities are presented in Table 5. Furthermore, Table 6 indicates the specific amino acid residues within the receptors 2QMJ and 2QVA binding sites.

Absorption, Distribution, Metabolism, Excretion, and Toxicity (ADMET) prediction

Compounds exhibiting superior binding affinity were subject to further analysis using predictive online software platforms, which provide insights into pharmacokinetics, physicochemical characteristics, and drug-likeness. According to Lipinski's Rule of Five, all evaluated compounds met the criteria, although 12 compounds presented with a single violation, whereas the remaining 10 compounds conformed entirely to the rule. It is generally considered that a compound with two or more unsuitable against Lipinski's rule might be less suitable as an orally administered drug. Notably, all compounds with the most favorable binding affinity values displayed characteristics similar to orally administered drugs. These attributes are significantly advantageous for patient treatment, offering ease of administration and avoiding the discomfort associated with non-oral delivery methods. Table 7 displays the compound that emerged as the most promising candidate for its ADMET profile.

Discussion

Qualitative phytochemical analysis revealed the presence of flavonoids, phenolic compounds, terpenoids, steroids, and alkaloids in the methanol and ethyl acetate extracts of *E. sumatrensis*. Conversely, the *n*-hexane extract was only terpenoids and steroids (Table 1). The methanol extract of *E. sumatrensis* also contained tannins, alkaloids, and saponins. The ethyl acetate extract contained flavonoids, steroids, terpenoids, and saponins, whereas the n-hexane extract contained steroids and terpenoids (Aiyelaagbe et al. 2016). Previous research reported that ethanol extract of *E. sumatrensis* contains tannins, saponins, flavonoids, steroids, and glycosides (Jack and Okorosaye-Orubite 2008). Further investigations are recommended to explore a broader range of solvents to enhance the extracted potential phytochemicals.

The results of the qualitative phytochemical assessment did not indicate the presence of tannins; however, the quantitative assay showed the presence of tannins (Table 2). Discrepancies between qualitative and quantitative results could be due to differences in sensitivity and specificity, different test conditions, and the matrix effects of the sample. Quantitative assays of the vanillin-HCl increased reliability and sensitivity, enabling the detection of tannins that may not be identified in qualitative screenings.

Table 4. Antioxidant activities of *Erigeron sumatrensis* leave

Extract	IC_{50} value in the method of		
	DPPH μg/mL	FRAP μg/mL	ABTS μg/mL
n-hexane	353.50	131.31	94.60
Ethyl acetate	236.78	93.52	81.10
Methanol	212.84	70.19	57.67

Table 5. Identification of metabolites in methanol extract of *Erigeron sumatrensis* by GC-MS

Compounds name	PubChem CID	Binding score (kcal/mol)	
		2QMJ	2QV4
Cucurbitacin b, 25-desacetoxy-	5363626	**-8.3**	**-10.6**
ß-Sitosterol	222284	**-8.3**	**-9.3**
α-Amyrin	73170	**-7.8**	**-10.9**
9,10-Secocholesta-5,7,10(19)-triene-3,24,25- triol, (3ß,5Z,7E)-	5372266	-7.4	-8.9
Lupeol	259846	-6.9	**-9.3**
Taylorione	12152394	-6.9	-6.8
trans-Za-Bisabolene epoxide	5363099	-6.6	-6.9
Pterin-6-carboxylic acid	135403803	-6.2	-7
cis-ß-Farnesene	480483983	-6.1	-5.7
2,3-Dehydro-4-oxo-ß-ionol	5373836	-5.9	-7.1
2-Methoxy-4-vinylphenol	332	-5.9	-5.6
Farnesyl bromide	5366048	-5.9	-6.6
Phytol	5280435	-5.9	-6.1
Caryophyllene oxide	439985448	-5.7	-7.1
Z-3-Hexadecen-7-yne	5362886	-5.7	-5.8
Phenol, 2-methoxy-5-(1-propenyl)-, (E)-	319246226	-5.6	-5.8
Methyl 8,11,14-heptadecatrienoate	85978449	-5.5	-5.7
Methyl 9-cis,11-trans-octadecadienoate	11748436	-5.5	-5.3
1H-Cycloprop[e]azulen-7-ol, decahydro- 1,1,7-trimethyl-4-methylene-, [1ar(1aa,4aa,7ß,7aß,7ba)]-	6432640	-5.3	-7.2
Hexadecanoic acid, methyl ester	8181	-5.1	-5.3
E-2-Tetradecen-1-ol	5353006	-5	-5.1
1,4-Cyclohexanediol, (Z)-, TMS derivative	11162	-5	-4.7
Acarbose (Control)	-	**-7.8**	**-9.2**

Note: Bold compounds indicated the best binding score

Table 6. Description of the amino acid residue of 2QMJ and 2QVA receptors

Ligand	Structure	Amino acid residues (2QMJ)	Amino acid residues (2QV4)
Acarbose	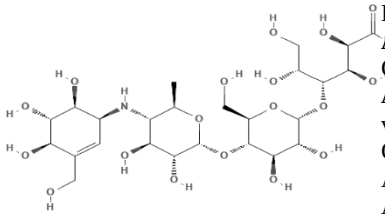	Hydrogen Bond: **ASP203, ARG526, ASP542** Carbon Hydrogen Bond: **HIS600, ASP327**, ASP443 van der Waals: PHE450, SER448, GLY541 TRP539, ARG598, ASP571, TRP441, ILE364, ILE328, ALA576, THR544, THR205, ASN207 Sulfur: MET444 Pi-Alkyl: TYR299, PHE575, TRP406	Hydrogen Bond: **TRP59,** GLN63, ALA106, VAL107, ASN105, **THR163**, ASP300 Carbon Hydrogen Bond: **GLU233**, ASP197, TYR62, GLY164 van der Waals: ARG195, HIS299, TRP58, **TYR151**, ILE235, LEU162, HIS201, **LYS200,** HIS101, ALA198, LEU165, GLY104, ILE51 Unfavorable bond: **HIS305**
Cucurbitacin b, 25-desacetoxy-	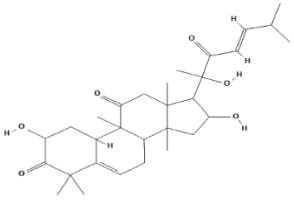	Hydrogen Bond: THR205 van der Waals: ASP474, LEU473, ARG202, LYS480, **ASP203,** MET444, PHE450, **ASP542, ARG526**, TRP406, TYR299, PHE575, GLN603. GLY602, TYR605, ALA576, TYR214, THR204	Carbon Hydrogen Bond: VAL107 van der Waals: TYR52, VAL49, SER108, GLY164, ALA50, GLY104, GLN63, **THR163,** LEU165, TYR62, ASN53, ALA106, ASN105, ILE51 Alkyl and Pi-Akyl: **TRP59, HIS305,** TRP58
ß-Sitosterol	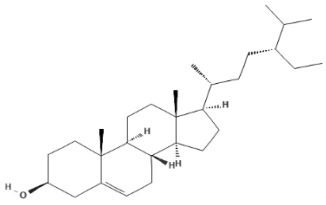	Hydrogen Bond: GLN603 Alkyl and Pi-Akyl: PHE575, ALA576, TRP406, PHE450	Hydrogen Bond**:** GLN63 van der Waals: **HIS305**, **THR163**, TRP58, **TRP59,** ARG195, ASP300, ASP197, ALA198, ALA307, GLY306 Alkyl dan Pi-Alkyl: LEU162, LEU165, TYR62, ILE235, **TYR151**
α-Amyrin	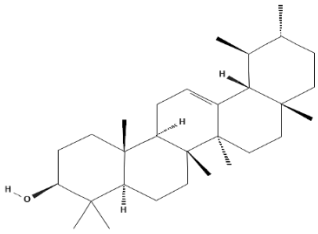	Carbon Hydrogen Bond: **ASP203** Van der Waals: PHE450, THR204, THR205, ASN207, LEU577, THR544, TYR605, PHE575, **ASP542, ARG526**, TYR299, MET444	Van der Waals: **TRP58, THR163, HIS305,** TRP59, ASP300, HIS101, ASP197, ARG195, **GLU233**, ALA198, ILE234, **TYR151,** GLY306, ALA307 Alkyl and Pi-Akyl: HIS201, LEU165, TYR62, LEU162

Note: "Bold" The protein active side

Phenolic and flavonoid constituents are recognized as principal natural components with antioxidant activity of plant-based sources, which have beneficial health advantages (Ahmed et al. 2022). Among the various parts of *E. sumatrensis*, the leaves have the highest phenolic content, suggesting a potential antioxidant activity. Previous research noted that cultivated and wild fruits with high total phenolic content showed good antioxidant properties (Phuyal et al. 2020).

The current investigation focused on the methanol extract with higher bioactive content than other extracts (Table 2). Methanol, characterized by its high polarity, effectively dissolves a wide range of polar and semi-polar compounds. This property renders it a highly suitable solvent for extracting various bioactive compounds, including, but not limited to, flavonoids, alkaloids, and polyphenols (Truong et al. 2019). GC-MS findings revealed that the highest chemical compound was phytol (19.32%), at peak number 16. Phytol, an acyclic diterpene ubiquitously synthesized by photosynthetic organisms such as plants, algae, and cyanobacteria with its array of biological activities, including cytotoxic, antibacterial, antioxidant, and anti-inflammatory properties, which are of significant pharmaceutical interest. Additionally, the compound recorded at peak number 24, identified as lupeol and categorized under pentacyclic triterpenoids, is routinely found in various fruits and vegetables. Lupeol has several health benefits, including anticancer, antimicrobial, antidiabetic, cardioprotective, and hepatoprotective effects (Hashmi et al. 2018; Huang et al. 2021; Kim and Lee 2021; Li et al. 2022).

Flavonoids, a distinctive subclass of phenolic compounds, are extensively investigated for their antioxidant capabilities and are commonly found in vegetables, fruits, nuts, seeds,

stems, and flowers. The mechanism underlying the antioxidant effect of flavonoids involves their capacity to neutralize reactive oxidative species by hydrogen atom donation or single-electron transfer to free radicals. The total phenolic content showed a high correlation with antioxidant activity. Antioxidant activity, as indicated by the IC_{50} value in the DPPH radical scavenging assay, was considered modest (212.84 µg/mL). However, the IC50 values in the FRAP and the ABTS assays were 57.67 µg/mL and 70.19 µg/mL, respectively. It is indicated that the methodological approach significantly influences the quantification of antioxidant activity, which varies according to the specific reagents used in each assay. The methanol extract of *E. sumatrensis* leaves exhibited antioxidant properties, aligned with previous research demonstrating the potent antioxidant activity of an ethanol extract (IC_{50} = 84.018 µg/mL). The antioxidant potential of the ethyl acetate extract was comparatively lower (IC_{50} = 311,346 µg/mL) than that of methanol extract. It is widely known that an increased phenolic content increases antioxidant activity (Phuyal et al. 2020; Muflihah et al. 2021; Mustikasari et al. 2024).

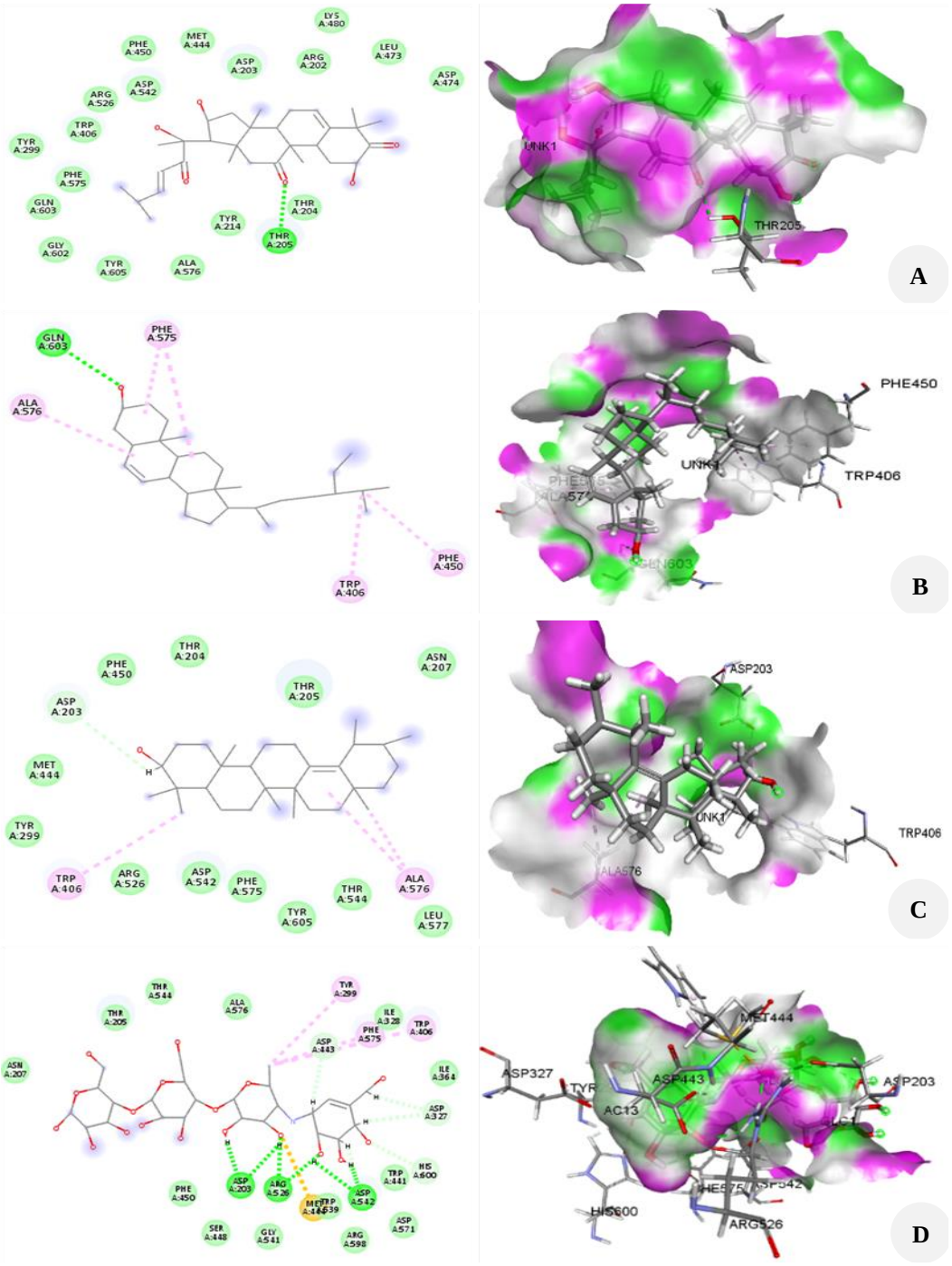

Figure 3. 2D & 3D interaction of 2QMJ with ligand. A. Cucurbitacin b, 25-desacetoxy-; B. β-sitosterol; C. α-amyrin; and D. Acarbose with human lysosomal α-glucosidase (PDB ID. 2QMJ) (Pose predicted by BIOVIA Discovery Studio)

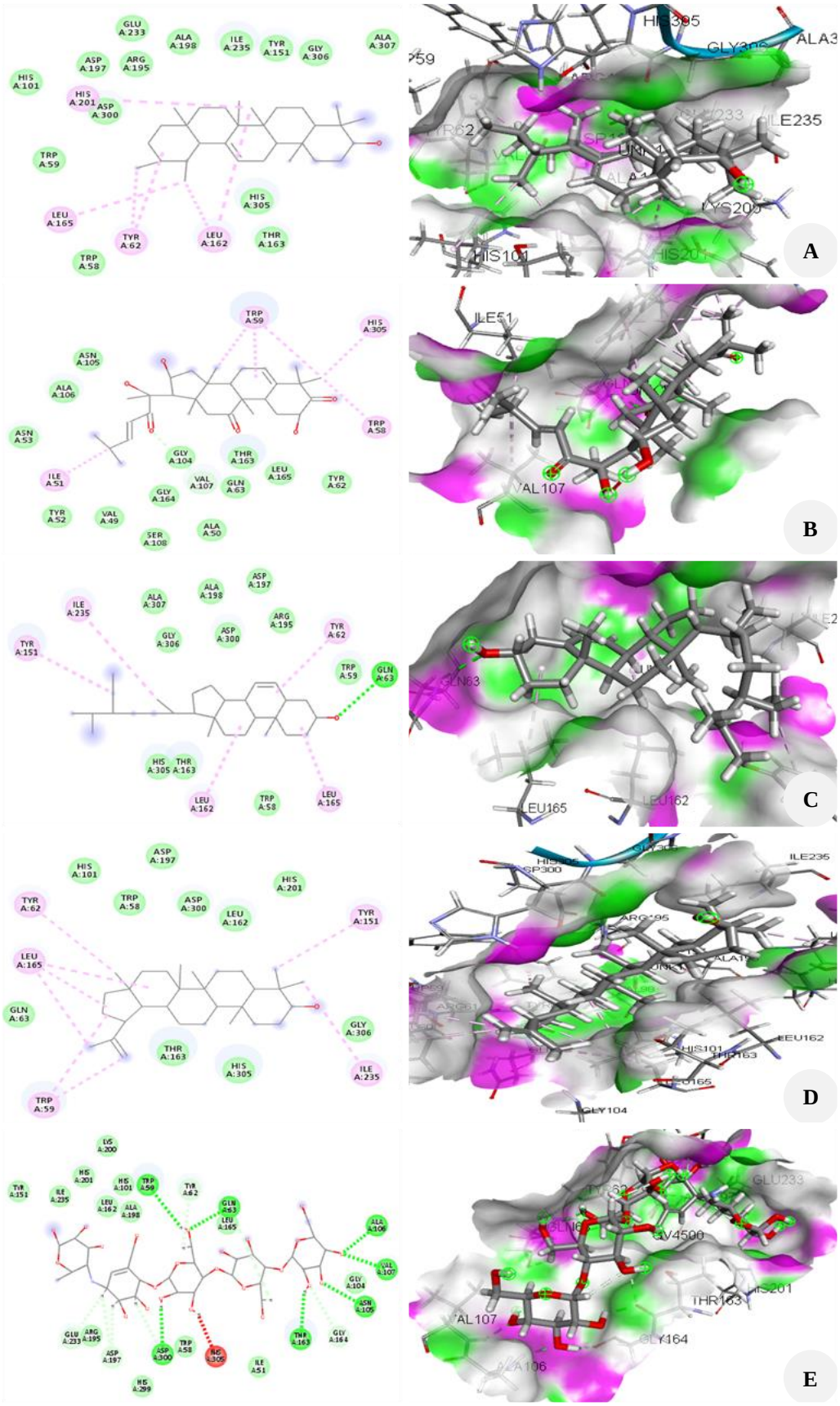

Figure 4. 2D & 3D interaction of 2QV4 with ligand. A. α-amyrin; B. Cucurbitacin b, 25-desacetoxy-; C. β-sitosterol; D. Lupeol; and E. Acarbose with α-amylase (PDB ID. 2QV4) (Pose predicted by BIOVIA Discovery Studio)

Table 7. ADMET prediction of the best compound parameters

	Parameters	Cucurbitacin b, 25-desacetoxy-	ß-Sitosterol	α-Amyrin	Lupeol
Absorption	Water solubility	Moderately soluble	Poorly soluble	Poorly soluble	Poorly soluble
	Log Kp (Skin Permeation)	-6.8 cm/s	-2.2 cm/s	-2.51 cm/s	-1.90 cm/s
	GI absorption	83.478 % (High)	94.886 % (Low)	94.444 % (Low)	97.882 % (Low)
Distribution	BBB	No	No	No	No
	P-gp substrate	Yes	No	No	No
	VDss (human) log L/kg	-0.094	0.24	0.318	0.023
Metabolism	CYP1A2 inhibitors	No	No	No	No
	CYP2C19 inhibitors	No	No	No	No
	CYP2C9 inhibitors	No	No	No	No
	CYP2D6 inhibitors	No	No	No	No
	CYP3A4 inhibitors	Yes	Yes	No	No
Excretion	Excretion Total Clearance (log mL/min/kg)	0.322	0.628	0.119	0.153
	Renal OCT2 substrate	No	No	No	No
Toxicity	AMES toxicity	No	No	No	No
	Maximum tolerated dose (human) (log mg/kg/day	-1.013	-0.555	-0.442	-0.303
	Oral Rat Acute Toxicity (LD_{50})	3,265	2,326	2,217	2,594
	Oral Rat Chronic Toxicity (LOAEL)	1,763	0.829	0.854	0.917
	Hepatotoxicity	No	No	No	No
	Skin Sensitization	No	No	No	No

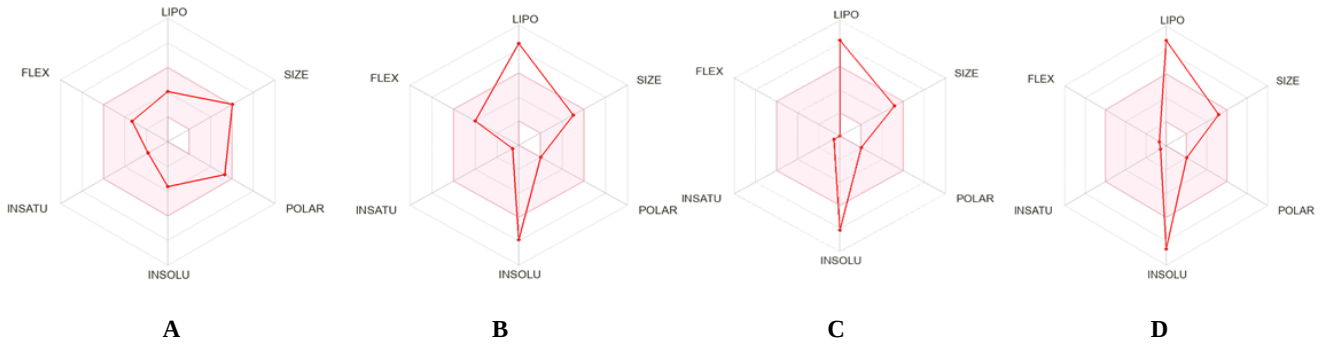

Figure 5. Bioavailability RADAR of best-docked compounds: A. Cucurbitacin b, 25-desacetoxy-; B. ß-Sitosterol; C. α-Amyrin; D. Lupeol

Antioxidant activities exhibited by the methanol, ethyl acetate, and *n*-hexane extracts of *E. sumatrensis* leaves were different (Table 4.). The methanol extract demonstrated a markedly higher antioxidant capacity as determined by several methods, specifically DPPH, FRAP, and ABTS, with corresponding IC_{50} values of 212.84 µg/mL, 70.19 µg/mL, and 57.67 µg/mL. The increased antioxidant activity correlates with the total phenolic and flavonoid content, which was found to be most abundant in the methanol extract compared to others. These findings align with previous research attributing a significant role to flavonoids and phenols in correlation to antioxidant activity. A previous study on *Clerodendrum minahassae* leaves showed that IC_{50} values of the methanol, *n*-hexane, ethyl acetate, and aqueous extract were 179.5 µg/mL, 752.92 µg/mL, 227.39 µg/mL, and 475.04 µg/mL, respectively (Suoth et al. 2022).

In the case of *Piper umbellatum* L., the methanol extract was identified as the most potent antioxidant with an IC50 of 1.2 µg/mL, while IC50 of vitamin C as a positive control was 1.7 µg/mL) and other extracts, including water-methanol (IC_{50} = 4.5 µg/mL), methylene chloride (IC_{50} = 5.9 µg/mL), ethyl acetate (IC_{50} = 8.0 µg/mL), 4-nerolidylcatechol (IC_{50} = 8.6 µg/mL), and the sterol fraction (IC_{50} = 12.5 µg/mL) (Ahmad et al. 2022). These findings suggest that the methanol extract might be able to extract higher antioxidant compounds than other solvents. It is consistent with the premise that polar solvents exhibit superior antioxidant activity compared to semi-polar or non-polar solvents (Fioroni et al. 2023).

Computational in silico approaches and molecular structuring are invaluable in searching for novel pharmacological agents. Compounds isolated from the methanol extract interact with α-glucosidase and α-amylase enzymes. A more negative value signifies a lower binding energy, reflecting a higher affinity for the enzyme's active site, as exemplified by acarbose, utilized as a positive control in the studies (Ahmed et al. 2022; Khan et al. 2023). The compounds cucurbitacin B, 25-desacetoxy- and β-sitosterol were identified as having the strongest binding affinity towards α-glucosidase, with docking scores of -8.3 kcal/mol, paralleling acarbose's control value of -7.8

kcal/mol at the binding site coordinates of 2QMJ X:12.9994, Y:47.0401, Z:25.5004 in Angstrom units. Furthermore, α-amyrin exhibited the highest binding affinity to α-amylase with a docking score of -10.9 kcal/mol, surpassing acarbose's control value of -9.2 kcal/mol, followed by cucurbitacin B, 25-desacetoxy- at -10.6 kcal/mol, and β-sitosterol at -9.3 kcal/mol. The docking site for α-amylase is disclosed with receptor coordinates 2QV4 X: -23.1437, Y: -6.7576, Z: -7.0051, with dimensions measured in Angstroms, as demonstrated in Table 5. Figures 3 and 4 elucidate that within the protein-ligand binding interactions, hydrophobic bonds predominately contribute to the stability of the interaction, with the presence of hydrogen bonds being minimal by comparison. Moreover, the efficacy of ligand binding is characterized by the capacity of the ligand molecule to engage with the receptor's amino acids. Ashraf et al. (2021) have noted the variety of interactions stabilizing the receptor-ligand complex, encompassing hydrogen bonds, carbon-hydrogen bonds, van der Waals interactions, as well as alkyl and pi-alkyl bonds, as detailed in Table 6.

The interaction of acarbose with the catalytic domain of α-glucosidase (PDB ID: 2QMJ) is characterized by a complex of hydrogen bonds formed with amino acid residues ASP327, ASP542, and ARG526 and augmented by carbon-hydrogen bonding at HIS600 and ASP327. The architecture of the sugar-binding site is further delineated by additional residues, specifically ASP443, TYR299, ILE238, ILE364, TRP441, and MET444, as evidenced in the research by Sim et al. (2008) elaborated by Rashid et al. (2022). The ligands under study show van der Waals forces and alkyl and pi-alkyl bonding types. Traditional hydrogen bond interactions extend to other active site constituents for acarbose, including cucurbitacin B, 25-desacetoxy- and β-sitosterol. Concurrently, acarbose and α-amyrin form carbon-hydrogen bonds. The amino acid reoccurrence analysis identifies cucurbitacin B, 25-desacetoxy- as the most promising compound in terms of therapeutic potential, given its superior negative binding affinity and the prevalence of its bonds at the active site, involving the residues ASP203, ASP542, and ARG526. The specific details concerning the amino acid residues of α-glucosidase at 2QMJ are presented in Table 6.

The interaction of acarbose with α-amylase (PDB ID: 2QV4) is facilitated by a large number of bonding interactions, including hydrogen bonds with TRP59 and THR163, as well as van der Waals interactions with TYR151 and LYS200. Additional binding is achieved through carbon bonds at GLU233, while HIS305 is involved in unfavorable bonding (Akshatha et al. 2021; Abchir et al. 2023). Acarbose engages traditional hydrogen bonding at the active site of the α-amylase receptor with TRP59 and THR163. The ligand β-sitosterol, however, does not interact through the active site of the α-amylase receptor. Acarbose is observed to form carbon-hydrogen bonds at GLU233 within the protein's catalytic domain, whereas cucurbitacin B, 25-desacetoxy-, establishes carbon bonds outside the active site; all studied ligands, nevertheless, participate in van der Waals interactions. A comprehensive amino acid residue analysis indicates that α-amyrin emerges as the compound of highest therapeutic interest due to its enhanced negative binding affinity and robust active binding with α-amylase at sites including TRP59, THR163, HIS305, GLU233, and TYR151. A detailed enumeration of additional interactive amino acid residues is presented in Table 6.

Cucurbitacin B, 25-desacetoxy- is easily soluble, whereas other compounds such as β-sitosterol, α-amyrin, and lupeol show more difficult solubility. In the pharmacokinetic context, a compound's solubility is crucial to its bioavailability. Drug solubility is directly correlated with the rate of drug absorption, which is critical to ensuring that a pharmaceutical agent is adequately absorbed to provide its intended therapeutic effects. Ferreira and Andricopulo (2019) noted that solubility significantly affects the kinetics of drug distribution in biological systems. Lipophilic compounds bind extensively to plasma proteins, facilitating rapid tissue distribution, and predominantly undergo hepatic metabolism. Highly soluble (hydrophilic) drugs typically exhibit restricted distribution and are primarily excreted via renal mechanisms. The bioavailability radar, presented in Figure 5, visually represents the pharmacokinetic profile for the compound with the most favorable binding affinity.

According to Santoso (2019), administering α-amyrin at 10, 30, and 100 mg/kg in rodent models reduced blood glucose, total cholesterol, and serum triglycerides. Furthermore, α-amyrin significantly reduced the surge in plasma glucose levels during oral glucose tolerance assays. Analytical assays, including plasma insulin measurements and histopathological assessments of pancreatic tissue, have demonstrated the beneficial impact of α-amyrin on pancreatic beta-cell integrity. Complementary to these findings, molecular docking analyses indicate that the methanol extract from *E. sumatrensis* harbors constituents capable of inhibiting α-glucosidase and α-amylase, thereby having the extract's potential as a source for naturally derived antidiabetic agents. Considering the expansive distribution of the *E. sumatrensis* species, particularly in the Gayo Highlands, the abundance of this species has the potential for developing antidiabetic therapy.

Based on pharmacological evaluations and molecular docking, the methanol fraction of the leaves of *E. sumatrensis* has a therapeutic activity for T2DM. Qualitative phytochemical screenings have revealed that the *E. sumatrensis* leaf extract contained flavonoids, phenolics, terpenoids, steroids, and alkaloids. Quantitative phytochemical analysis showed that the methanol extract contained the highest total phenolic (5945.45 mg GAE/g). The methanol extract also has antioxidant activity. These findings indicate that *E. sumatrensis* leaves had the potential as antioxidants, with a particular emphasis on managing T2DM.

Molecular docking studies have identified the compounds exhibiting superior binding affinities relative to a standard reference, with acarbose as the positive control (with a binding energy of -7.8 kcal/mol). Three compounds are potential as α-glucosidase inhibitors targeting the enzyme with PDB ID: 2QMJ, i.e., cucurbitacin B, 25-deacetoxy-; β-sitosterol; and α-amyrin, and cucurbitacin B, 25-deacetoxy-, is being the most potential. These three compounds also

have the potential to inhibit α-amylase (PDB ID: 2QV4), with α-amyrin being the most potent. ADMET profiling of the potential candidates indicates good compliance with Lipinski's Rule of Five, suggesting their viability as orally administered therapeutics. These findings provide compelling evidence for the potential of *E. sumatrensis* as a valuable source for developing novel therapeutics targeting Type-2 diabetes mellitus.

ACKNOWLEDGEMENTS

The authors thank Indonesia's Ministry of Education, Culture, Research, and Technology for funding this study through *Beasiswa Pendidikan Indonesia* (BPI), the Indonesian Education Scholarship for the *Penyelesaian Studi S3* Scheme.

REFERENCES

Abchir O, Daoui O, Nour H, Yamari I, Elkhattabi S, Errougui A, Chtita S. 2023. Exploration of *Cannabis* constituents as potential candidates against diabetes mellitus disease using molecular docking, dynamics simulations, and ADMET investigations. Sci Afr 21: e01745. DOI: 10.1016/j.sciaf.2023.e01745.

Abu-Izneid T, Rauf A, Saleem M, Mansour N, Abdelhady MIS, Ibrahim MM, Patel S. 2020. Urease inhibitory potential of extracts and active phytochemicals of *Hypochaeris radicata* (Asteraceae). Nat Prod Res 34 (4): 553-557. DOI: 10.1080/14786419.2018.1489387.

Ahmad I, Ahmed S, Akkol EK, Rao H, Shahzad MN, Shaukat U, Basit A, Fatima M. 2022. GC-MS profiling, phytochemical and biological investigation of aerial parts of *Leucophyllum frutescens* (Berl.) I.M. Johnst (Cenizo). S Afr J Bot 148: 200-209. DOI: 10.1016/j.sajb.2022.04.038.

Ahmed M, Khan K-U-R, Ahmad S, Aati HY, Sherif AE, Ashkan MF, Alrahimi J, Motwali EA, Tousif MI, Khan MA, Hussain M, Umair M, Ghalloo BA, Korma SA. 2022. Phytochemical, antioxidant, enzyme inhibitory, thrombolytic, antibacterial, antiviral and in silico studies of *Acacia jacquemontii* leaves. Arab J Chem 15 (12): 104345. DOI: 10.1016/j.arabjc.2022.104345.

Aiyelaagbe OO, Oguntoye SO, Hamid AA, Ogundare AM, Ojo DB, Ajao A, Owolabi NO. 2016. GC-MS Analysis, antimicrobial and antioxidant activities of extracts of the aerial parts of *Conyza sumatrensis*. J Appl Sci Environ Manag 20 (1): 103. DOI: 10.4314/jasem.v20i1.13.

Akshatha JV, SantoshKumar HS, Prakash HS, Nalini MS. 2021. In silico docking studies of α-amylase inhibitors from the antidiabetic plant *Leucas ciliata* Benth. and an endophyte, *Streptomyces longisporoflavus*. 3 Biotech 11 (2): 51. DOI: 10.1007/s13205-020-02547-0.

Ali SI, Gopalakrishnan B, Venkatesalu V. 2017. Pharmacognosy, phytochemistry and pharmacological properties of *Achillea millefolium* L.: A review. Phytother Res 31 (8): 1140-1161. DOI: 10.1002/ptr.5840.

Al-Momani LA, Abu-Orabi ST, Hlail HM, Alkhatib RQ, Al-Dalahmeh Y, Al-Qudah MA. 2023. *Anthemis cotula* L. from Jordan: Essential oil composition, LC-ESI-MS/MS profiling of phenolic acids - flavonoids and in vitro antioxidant activity. Arab J Chem 16 (2): 104470. DOI: 10.1016/j.arabjc.2022.104470.

Al-Qahtani J, Abbasi A, Aati HY, Al-Taweel A, Al-Abdali A, Aati S, Yanbawi AN, Khan MA, Ghalloo BA, Anwar M, Khan K-u-R. 2023. Phytochemical, antimicrobial, antidiabetic, thrombolytic, anticancer activities, and in silico studies of *Ficus palmata* Forssk. Arab J Chem 16 (2): 104455. DOI: 10.1016/j.arabjc.2022.104455.

Ascari J, de Oliveira MS, Nunes DS, Granato D, Scharf DR, Simionatto E, Otuki M, Soley B, Heiden G. 2019. Chemical composition, antioxidant and anti-inflammatory activities of the essential oils from male and female specimens of *Baccharis punctulata* (Asteraceae). J Ethnopharmacol 234: 1-7. DOI: 10.1016/j.jep.2019.01.005.

Ashraf J, Mughal EU, Alsantali RI, Obaid RJ, Sadiq A, Naeem N, Ali A, Massadaq A, Javed Q, Javid A, Sumrra SH, Zafar MN, Ahmed SA. 2021. Structure-based designing and synthesis of 2-phenylchromone derivatives as potent tyrosinase inhibitors: In vitro and in silico studies. Bioorg Med Chem 35: 116057. DOI: 10.1016/j.bmc.2021.116057.

Asif M, Iqbal Z, Alam J, Majid A, Ijaz F, Ali N, Rahman IU, Hussain S, Khan A, Qadir G. 2020. Floristic inventory and biological spectra of Balakot, District Mansehra, Pakistan. Acta Ecol Sin 40 (3): 197-203. DOI: 10.1016/j.chnaes.2019.05.009.

Bakar F, Bahadir Acikara Ö, Ergene B, Nebioğlu S, Saltan Çitoğlu G. 2015. Antioxidant activity and phytochemical screening of some Asteraceae plants. Turk J Pharm Sci 12 (2): 123-132. DOI: 10.5505/tjps.2015.18209.

Bartolome AP, Villaseñor IM, Yang W-C. 2013. *Bidens pilosa* L. (Asteraceae): Botanical properties, traditional uses, phytochemistry, and pharmacology. Evid Based Complement Alternat Med 2013: 340215. DOI: 10.1155/2013/340215.

Boucheffa S, Sobhi W, Attoui A, Selli S, Kelebek H, Semmeq A, Benguerba Y. 2022. Effect of the main constituents of *Pistacia lentiscus* leaves against the DPPH radical and xanthine oxidase: Experimental and theoretical study. J Biomol Struct Dyn 40 (20): 9870-9884. DOI: 10.1080/07391102.2021.1936182.

Chandel V, Tripathi G, Nayar SA, Rathi B, Kumar A, Kumar D. 2022. In silico identification and validation of triarylchromones as potential inhibitor against main protease of severe acute respiratory syndrome coronavirus 2. J Biomol Struct Dyn 40 (19): 8850-8865. DOI: 10.1080/07391102.2021.1918255.

Chipiti T, Ibrahim MA, Singh M, Islam MS. 2017. In vitro α-amylase and α-glucosidase inhibitory and cytotoxic activities of extracts from *Cissus cornifolia* planch parts. Pharmacogn Mag 13 (Suppl 2): S329-S333. DOI: 10.4103/pm.pm_223_16.

Ernilasari, Walil K, Fitmawati, Roslim DI, Zumaidar, Saudah, Rayhannisa. 2021. Antibacterial activity of leaves, flowers, and fruits extract of *Etlingera elatior* from Nagan Raya district, Indonesia against *Escherichia coli* and *Staphylococcus aureus*. Biodiversitas 22 (10): 4457-4464. DOI: 10.13057/biodiv/d221039.

Erukainure OL, Otukile KP, Harejane KR, Salau VF, Aljoundi A, Chukwuma CI, Matsabisa MG. 2023. Computational insights into the antioxidant and antidiabetic mechanisms of cannabidiol: An in vitro and in silico study. Arab J Chem 16: 104842. DOI: 10.1016/j.arabjc.2023.104842.

Farahmandfar R, Ramezanizadeh MH. 2018. Oxidative stability of canola oil by *Biarum bovei* bioactive components during storage at ambient temperature. Food Sci Nutr 6 (2): 342-347. DOI: 10.1002/fsn3.560.

Ferreira LLG, Andricopulo AD. 2019. ADMET modeling approaches in drug discovery. Drug Discov Today 24 (5): 1157-1165. DOI: 10.1016/j.drudis.2019.03.015.

Fioroni N, Mouquet-Rivier C, Meudec E, Cheynier V, Boudard F, Hemery Y, Laurent-Babot C. 2023. Antioxidant capacity of polar and non-polar extract of four African green leafy vegetables and correlation with polyphenol and carotenoid contents. Antioxidants 12 (9): 1726. DOI: 10.3390/antiox12091726.

Frederick N, Mani JV. 2016. total phenolic content, total flavonoid content, total tannin content and antioxidant activity of *Musa acuminate*. J Intl Acad Res Multidiscip 4 (1): 300-308. DOI. 10.13140/RG.2.2.35749.09441.

Fu L, Zheng Y, Wang A, Zhang P, Ding S, Wu W, Zhou Q, Chen F, Zhao S. 2021. Identification of medicinal herbs in Asteraceae and Polygonaceae using an electrochemical fingerprint recorded using screen-printed electrode. J Herb Med 30: 100512. DOI: 10.1016/j.hermed.2021.100512.

Furi M, Al Basit N, Ikhtiarudin I, Utami R. 2020. Determination of total phenolics, flavonoids and test of antioxidant activity of Kedabu leaf extract and fraction (*Sonneratia ovata* Backer). Jurnal Farmasi Indonesia 12: 48-59. DOI: 10.35617/jfionline.v12i1.56. [Indonesian]

Gholam GM, Artika IM. 2023. Potential for molecular interactions in natural phytochemicals as Sap2 inhibitors of *Candida albicans*: An in silico approach. Jurnal Farmasi Udayana 11: 54-62. DOI: 10.24843/jfu.2022.v11.i02.p04. [Indonesian]

González-Zamora A, Ríos-Sánchez E, Pérez-Morales R. 2020. Conservation of vascular plant diversity in an agricultural and industrial region in the Chihuahuan Desert, Mexico. Glob Ecol Conserv 22: e01002. DOI: 10.1016/j.gecco.2020.e01002.

Hashmi WJ, Ismail H, Mehmood F, Mirza B. 2018. Neuroprotective, antidiabetic and antioxidant effect of *Hedera nepalensis* and Lupeol against STZ + AlCl3 induced rats model. Daru 26 (2): 179-190. DOI: 10.1007/s40199-018-0223-3.

Huang S, Mo C, Zeng T, Lai Y, Zhou C, Xie S, Chen L, Wang Y, Chen Y, Huang S, Gao L, Lv Z. 2021. Lupeol ameliorates LPS/D-GalN

induced acute hepatic damage by suppressing inflammation and oxidative stress through TGFbeta1-Nrf2 signal pathway. Aging 13 (5): 6592-6605. DOI: 10.18632/aging.202409.

Indriaty, Djufri, Ginting B, Hasballah K. 2023. Phytochemical screening, phenolic and flavonoid content, and antioxidant activity of Rhizophoraceae methanol extract from Langsa, Aceh, Indonesia. Biodiversitas 24 (5): 2865-2876. DOI: 10.13057/biodiv/d240541.

Jack IR, Okorosaye-Orubite K. 2008. Phytochemical analysis and antimicrobial activity of the extract of leaves of fleabane (*Conyza sumatrensis*). J Appl Sci Environ Manag 12 (4): 63-65. DOI: 10.4314/jasem.v12i4.55221.

Javeed A, Ahmed M, Sajid AR, Sikandar A, Aslam M, Ul Hassan T, Samiullah, Nazir Z, Ji M, Li C. 2022. Comparative assessment of phytoconstituents, antioxidant activity and chemical analysis of different parts of milk Thistle *Silybum marianum* L. Molecules 27 (9): 2641. DOI: 10.3390/molecules27092641.

Jhariya BL, Pawar M. 2024. Ethnomedicinal knowledge of Baiga and Gond Tribe and plant diversity in Jagmandal Forest, Mandla, India, with phytosociological diversity and utilization strategies. Asian J Ethnobiol 7: 13-21. DOI: 10.13057/asianjethnobiol/y070102.

Khan I, Rehman W, Rahim F, Hussain R, Khan S, Rasheed L, Alanazi AS, Hefnawy M, Alanazi MM, Shah SAA, Taha M. 2023. Synthesis, in vitro biological analysis and molecular docking studies of new thiadiazole-based thiourea derivatives as dual inhibitors of a-amylase and a-glucosidase. Arab J Chem 16 (9): 105078. DOI: 10.1016/j.arabjc.2023.105078.

Kim H, Lee DG. 2021. Lupeol-induced nitric oxide elicits apoptosis-like death within *Escherichia coli* in a DNA fragmentation-independent manner. Biochem J 478 (4): 855-869. DOI: 10.1042/BCJ20200925.

Li D, Guo Y-Y, Cen X-F, Qiu H-L, Chen S, Zeng X-F, Zeng Q, Xu M, Tang Q-Z. 2022. Lupeol protects against cardiac hypertrophy via TLR4-PI3K-Akt-NF-κB pathways. Acta Pharmacol Sin 43 (8): 1989-2002. DOI: 10.1038/s41401-021-00820-3.

Lopes AP, Bagatela BS, Rosa PCP, Nanayakkara DNP, Carvalho JCT, Maistro EL, Bastos JK, Perazzo FF. 2013. Antioxidant and cytotoxic effects of crude extract, fractions and 4-nerolidylcathecol from aerial parts of *Pothomorphe umbellata* L. (Piperaceae). Biomed Res Intl 2013: 206581. DOI: 10.1155/2013/206581.

Majid M, Farhan A, Asad MI, Khan MR, Hassan SSU, Haq I-U, Bungau S. 2022. An extensive pharmacological evaluation of new anti-cancer triterpenoid (nummularic acid) from *Ipomoea batatas* through in vitro, in silico, and in vivo studies. Molecules 27 (8): 2474. DOI: 10.3390/molecules27082474.

Masyudi, Hanafiah M, Rinidar, Usman S, Marlina. 2022. Phytochemical screening and GC-MS analysis of bioactive compounds of *Blumea balsamifera* leaf extracts from South Aceh, Indonesia. Biodiversitas 23 (3): 1344-1352. DOI: 10.13057/biodiv/d230319.

Muflihah YM, Gollavelli G, Ling Y-C. 2021. Correlation study of antioxidant activity with phenolic and flavonoid compounds in 12 Indonesian indigenous herbs. Antioxidants 10 (10): 1530. DOI: 10.3390/antiox10101530.

Mustikasari K, Santoso M, Abu Bakar MF, Fatmawati S. 2024. Antioxidant, α-glucosidase inhibitory, and cytotoxic activities of *Mangifera rufocostata* extract and identification of its compounds by LC-MS/MS analysis. Arab J Chem 17 (1): 105391. DOI: 10.1016/j.arabjc.2023.105391.

Nikolić M, Stevović S. 2015. Family Asteraceae as a sustainable planning tool in phytoremediation and its relevance in urban areas. Urban For Urban Green 14 (4): 782-789. DOI: 10.1016/j.ufug.2015.08.002.

Nuraskin C, Marlina, Idroes R, Soraya C, Djufri. 2020. Identification of secondary metabolite of laban leaf extract (*Vitex pinnata* l) from geothermal areas and non-geothermal of agam mountains in Aceh Besar, Aceh province, Indonesia. Rasayan J Chem 13 (1): 18-23. DOI: 10.31788/RJC.2020.1315434.

Nurmilasari, Ginting B, Helwati H. 2017. Isolation of antioxidant compounds of methanol extract of Nutmeg leaves (*Myristica fragrans* Houtt). Jurnal Natural 17 (1): 49-57. DOI: 10.24815/jn.v17i1.6998. [Indonesian]

Phuyal N, Jha PK, Raturi PP, Rajbhandary S. 2020. Total phenolic, flavonoid contents, and antioxidant activities of fruit, seed, and bark extracts of *Zanthoxylum armatum* DC. ScientificWorldJournal 2020: 8780704. DOI: 10.1155/2020/8780704.

Raharjo OW, Raharjo D, Permatasari DAI. 2023. Determination of flavonoid content and antioxidant activity test of red spinach leaves using ABTS and FRAP methods. Jurnal Farmasi dan Kesehatan Indonesia 3 (2): 126-137. DOI: 10.61179/jfki.v3i2.431. [Indonesian]

Rashid F, Javaid A, Mahmood-ur-Rahman, Ashfaq UA, Sufyan M, Alshammari A, Alharbi M, Nisar MA, Khurshid M. 2022. Integrating pharmacological and computational approaches for the phytochemical analysis of *Syzygium cumini* and its antidiabetic potential. Molecules 27 (17): 5734. DOI: 10.3390/molecules27175734.

Rolnik A, Olas B. 2021. The plants of the Asteraceae family as agents in the protection of human health. Intl J Mol Sci 22 (6): 3009. DOI: 10.3390/ijms22063009.

Ruiz-Reyes E, Mendoza-Cevallos MA, Polanco-Moreira AP, Segovia-Cedeño DG, Alcivar-Cedeño UE, Dueñas-Rivadeneira A. 2022. Phytochemical study of the plant species *Bidens pilosa* L. (Asteraceae) and *Croton floccosus* (Euphorbiaceae). F1000Res 11: 702. DOI: 10.12688/f1000research.112653.1.

Rustaiyan A, Faridchehr A. 2021. Constituents and biological activities of selected genera of the Iranian Asteraceae family. J Herb Med 25: 100405. DOI: 10.1016/j.hermed.2020.100405.

Sadeer NB, Rocchetti G, Senizza B, Montesano D, Zengin G, Uysal A, Jeewon R, Lucini L, Mahomoodally MF. 2019. Untargeted metabolomic profiling, multivariate analysis and biological evaluation of the true mangrove (*Rhizophora mucronata* Lam.). Antioxidants 8 (10): 489. DOI: 10.3390/antiox8100489.

Santoso B. 2019. In silico study of selected molecules of sea cucumber as antimitotic using PyRx-Vina program. Indones J Pharm Sci Technol 1: 33-38. DOI: 10.24198/ijpst.v1i2.20210.

Sim L, Quezada-Calvillo R, Sterchi EE, Nichols BL, Rose DR. 2008. Human intestinal maltase-glucoamylase: Crystal structure of the n-terminal catalytic subunit and basis of inhibition and substrate specificity. J Mol Biol 375: 782-792. DOI: 10.1016/j.jmb.2007.10.069.

Sohag AAM, Hossain MT, Rahaman MA, Rahman P, Hasan MS, Das RC, Khan MK, Sikder MH, Alam M, Uddin MJ, Rahman MH, Tahjib-Ul-Arif M, Islam T, Moon IS, Hannan MA. 2022. Molecular pharmacology and therapeutic advances of the pentacyclic triterpene lupeol. Phytomedicine 99: 154012. DOI: 10.1016/j.phymed.2022.154012.

Soković M, Skaltsa H, Ferreira ICFR. 2019. Editorial: Bioactive phytochemicals in Asteraceae: Structure, function, and biological activity. Front Plant Sci 10: 1464. DOI: 10.3389/fpls.2019.01464.

Soleimani V, Delghandi PS, Moallem SA, Karimi G. 2019. Safety and toxicity of silymarin, the major constituent of milk thistle extract: An updated review. Phytother Res 33: 1627-1638. DOI: 10.1002/ptr.6361.

Suoth EJ, Datu O, Jayanti M, Wehantouw F. 2022. Phytochemical analysis and antioxidant test extracts and solvent fractions from Leilem leaf cream preparations (*Clerodendrum minahassae*). Chem Prog 15 (2): 56-62. DOI: 10.35799/cp.15.2.2022.44485. [Indonesian]

Tangkau MI, Fatimawali, Suoth EJ. 2023. Antioxidant activity of ethanol extract white Galangal stem (*Alpina galanga*) with ABTS method. Pharmacon 12 (3): 358-366. DOI: 10.35799/pha.12.2023.49216. [Indonesian]

Thabit RAS, Cheng X-R, Tang X, Sun J, Shi Y-H, Le G-W. 2015. Antioxidant and antibacterial activities of extracts from *Conyza bonariensis* growing in Yemen. Pak J Pharm Sci 28 (1): 129-134.

Timalsina D, Devkota HP. 2021. *Eclipta prostrata* (L.) l. (Asteraceae): Ethnomedicinal uses, chemical constituents, and biological activities. Biomolecules 11 (11): 1738. DOI: 10.3390/biom11111738.

Truong D-H, Nguyen DH, Ta NTA, Bui AV, Do TH, Nguyen HC. 2019. Evaluation of the use of different solvents for phytochemical constituents, antioxidants, and in vitro anti-inflammatory activities of *Severinia buxifolia*. J Food Qual 2019 (1): 8178294. DOI: 10.1155/2019/8178294.

Valdés-Tresanco MS, Valdés-Tresanco ME, Valiente PA, Moreno E. 2020. AMDock: A versatile graphical tool for assisting molecular docking with Autodock Vina and Autodock4. Biol Direct 15 (1): 12. DOI: 10.1186/s13062-020-00267-2.

Yahya M, Ginting B, Saidi N. 2021. In-vitro screenings for biological and antioxidant activities of water extract from theobroma cacao l. Pod husk: Potential utilization in foods. Molecules 26: 6915. DOI: 10.3390/molecules26226915.

Zhao Y, Li M, Wang X, Deng J, Zhang Z, Wang B. 2020. Influence of habitat on the phylogenetic structure of *Robinia pseudoacacia* forests in the eastern Loess Plateau, China. Glob Ecol Conserv 24: e01199. DOI: 10.1016/j.gecco.2020.e01199.